Generation of fundamental soliton
in the presence of initial linear chirp

TOMASZ KACZMAREK

Kielce University of Technology, al. 1000lecia PP 7, 25-314 Kielce,
e-mail: tkaczmar@eden.tu.kielce.pl

Generation of fundamental soliton in nonlinear optical fiber from chirped pulses of different initial shapes is discussed. Results of numerical calculations having in view solution of nonlinear Schrödinger equation for complex initial condition using split-step Fourier method are presented. Initial shape-dependent critical value of the chirp parameter is determined. Critical value is such a value of the chirp parameter at which generation of soliton in optical fiber is impossible.

Keywords: Split-step Fourier method, soliton, chirp, nonlinear Schrödinger equation.

1. Introduction

A fascinating manifestation of the fiber nonlinearity occurs through optical solitons, formed as a result of the interplay between the dispersive and nonlinear effects. The word soliton refers to special kinds of wave packets that can propagate undistorted over long distances. Solitons have been discovered in many branches of physics. In the context of optical fibers, not only are solitons of fundamental interest but they have also found practical applications in the field of fiber-optic communications.

Propagation of picosecond optical pulses in single-mode lossless fiber is described by the nonlinear Schrödinger (NLS) equation [1], [2]

$$i\frac{\partial A}{\partial z} - \frac{\beta_2}{2}\frac{\partial^2 A}{\partial T^2} + \gamma|A|^2 A = 0 \tag{1}$$

where z and T are the spatial and time coordinates, respectively, $A(z, T)$ is the slowly varying pulse envelope. Group velocity dispersion (GVD) is governed by $\beta_2 = (\mathrm{d}^2\beta)/(\mathrm{d}\omega^2)$, nonlinear parameter is defined as $\gamma = n_2\omega_0/cA_{\text{eff}}$ (n_2 is the nonlinear refractive index and A_{eff} is known as the effective core area). It is useful to normalize Eq. (1) by introducing three dimensionless variables [1], [2]

$$U = \frac{A}{\sqrt{P_0}}, \qquad \xi = \frac{z}{L_D}, \qquad \tau = \frac{T}{T_0}, \tag{2}$$

and write it in the form [1], [2]

$$i\frac{\partial U}{\partial \xi} - \mathrm{sgn}(\beta_2)\frac{1}{2}\frac{\partial^2 U}{\partial \tau^2} + N^2|U|^2 U = 0 \tag{3}$$

where P_0 is the peak power, T_0 – the width of the incident pulse, $L_D = T_0^2/|\beta_2|$ – the dispersion length. Parameter N is introduced as [1], [2]

$$N^2 = \frac{L_D}{L_{NL}} = \frac{\gamma P_0 T_0^2}{|\beta_2|}, \tag{4}$$

where $L_{NL} = 1/\gamma P_0$ is the nonlinear length. The parameter N can be eliminated from Eq. (3) by introducing $u = NU = \sqrt{\gamma L_D}\,A$. Equation (3) then takes the standard form of the NLS equation [1], [2]

$$i\frac{\partial u}{\partial \xi} + \frac{1}{2}\frac{\partial^2 u}{\partial \tau^2} + |u|^2 u = 0, \tag{5}$$

where the choice $\mathrm{sgn}(\beta_2) = -1$ has been made to focus on the case of anomalous GVD. Equation (5) has analytical solution of the form [1], [2]

$$u(\xi,\tau) = \sec\left[h(\tau)\right]\exp\left(\frac{i\xi}{2}\right). \tag{6}$$

It can be obtained by solving standard form of the NLS equation using the inverse scattering method. In the context of optical fibers, the solution (6) indicates that if a hyperbolic-secant pulse, whose width T_0 and the peak power P_0 are chosen such that $N = 1$ in Eq. (4), is launched inside an ideal lossless fiber, the pulse will propagate undistorted without change in shape for arbitrary long distances. It is this feature of the fundamental solitons that makes them attractive for optical communication systems.

As pulses emitted from laser sources are often chirped, it is important to consider the effect of initial frequency chirp on soliton formation. The chirp can be detrimental simply because it superimposes on the self-phase modulation (SPM) induced chirp and disturbs the exact balance between the GVD and SPM effects necessary for solitons. Its effect on soliton formation can be studied by solving Eq. (5) numerically with an input amplitude [1], [2]

$$u(0, \tau) = N \sec\left[h(\tau)\right] \exp\left(-\frac{iC\tau^2}{2}\right) \tag{7}$$

in the case of hyperbolic-secant and [1], [2]

$$u(0, \tau) = N \exp\left(-\frac{\tau^{2m}}{2}\right) \exp\left(-\frac{iC\tau^2}{2}\right) \tag{8}$$

in the case of Gaussian and super-Gaussian initial shape (C is the chirp parameter). For $C > 0$ the instantaneous frequency increases linearly from the leading to the trailing edge of the pulse (up-chirp) while the opposite occurs (down-chirp) for $C < 0$. It is common to refer to the chirp as positive or negative depending on whether C is positive or negative. The chirp parameter C reaches the critical value C_{cr} if the stationary peak amplitude $|u|_{max, \text{ sationary}}$ of the fundamental soliton is equal to zero.

2. Method

The evaluation of C_{cr} can be divided into three stages. At the first stage the temporary envelope variability of the pulse with respect to the propagation distance is determined. For this purpose the NLS equation (5) should be solved for initial condition (7) or (8). The NLS equation is a nonlinear partial differential equation that does not generally lend itself to analytic solutions except for some specific cases in which the inverse scattering method can be employed. A numerical approach is therefore often necessary for an understanding of the nonlinear effects in optical fibers. A large number of numerical methods can be used for this purpose. The one method that has been used extensively to solve the pulse propagation problem in nonlinear dispersive media is the split-step Fourier (SSF) method. The relative speed of this method compared with most finite-difference schemes can be attributed in part to the use of the fast Fourier transform (FFT) algorithm. To understand the philosophy behind the SSF method it is useful to write Eq. (5) formally in the form [1]

$$\frac{\partial u}{\partial \xi} = (D + N)u, \tag{9}$$

where D is a differential operator that accounts for dispersion in a linear medium and N is a nonlinear operator that governs the effect of fiber nonlinearity on pulse propagation. These operators are given by [1]

$$D = \frac{i}{2}\frac{\partial^2}{\partial \tau^2}, \qquad N = i|u|^2. \tag{10}$$

In general, dispersion and nonlinearity act together along the length of the fiber. The SSF method obtains an approximate solution by assuming that in propagating the optical field over a small distance $\Delta\xi$, the dispersive and nonlinear effects can be presented to act independently. More specifically, propagation from ξ to $\xi + \Delta\xi$ is carried out in two steps. In the first step, the nonlinearity acts alone, and $D = 0$ in Eq. (9). In the second step, dispersion acts alone, and $N = 0$ in equation (9). Mathematically, [1]

$$u(\xi + \Delta\xi,\, \tau) \approx \exp(\Delta\xi D)\exp(\Delta\xi N)u(\xi,\, \tau). \tag{11}$$

The exponential operator $\exp(\Delta\xi D)$ can be evaluated in the Fourier domain using the prescription [1]

$$\exp(\Delta\xi D)\exp(\Delta\xi N)u(\xi,\, \tau) \;=\; F^{-1}\left\{\exp\left[\Delta\xi D(i\omega)\right]F\left[\exp(\Delta\xi N)u(\xi,\, \tau)\right]\right\}, \tag{12}$$

where F denotes the Fourier-transform operation, $D(i\omega)$ is obtained from Eq. (10) by replacing the differential operator $\partial/\partial\tau$ by $i\omega$, and ω is the frequency in the Fourier domain. As $D(i\omega)$ is just a number in the Fourier space, the evaluation of Eq. (12) is straightforward. The use of the FFT algorithm makes numerical evaluation of Eq. (12) relatively fast.

At the second stage, in order to calculate the stationary peak amplitude value $|u|_{\text{max, stationary}}$ of the envelope the peak amplitude as a function of the propagated distance $|u|_{\text{max}}(\xi)$ should be filtered. In this end an averaging filter with a variable window is used. The averaging filter functions in agreement with the following algorithm [3]

$$f_j \;=\; \frac{\displaystyle\sum_{i=j-n}^{j} |u|_{\text{max}}(\xi_i)}{n}, \tag{13}$$

where f_j is the j-th sample of the function $|u|_{\text{max}}(\xi)$ after the filtering, n is the variable length of the window of the filter. Function $|u|_{\text{max}}(\xi)$ is constructed such that, independently of the chirp parameter value C, it consists of 101 samples.

At the third stage C_{cr} is estimated. To that end a well known rational extrapolation algorithm [4] is used. The estimation of C_{cr} consists in seeking the zero of the curve $|u|_{\text{max, stationary}}(C)$.

3. Results

Making use of formula (12) computations were carried out for initial condition (7) (in the case of hyperbolic secant pulse) and condition (8) (in the case of Gaussian shape

– $m = 1$, in the case of super-Gaussian pulse of the first kind – $m = 2$, in the case of super-Gaussian pulse of the second kind – $m = 3$, and in the case of super-Gaussian pulse of the third kind – $m = 4$) for $\Delta\xi = 0.008$, $N = 1$ and for selected values of the chirp parameter C.

At the third stage of the evaluation of C_{cr} the following results were obtained:
– in the case of hyperbolic secant initial shape: $C_{cr+} = 1.626$, $C_{cr-} = -1.635$;
– in the case of Gaussian initial shape: $C_{cr+} = 1.807$, $C_{cr-} = -1.824$;
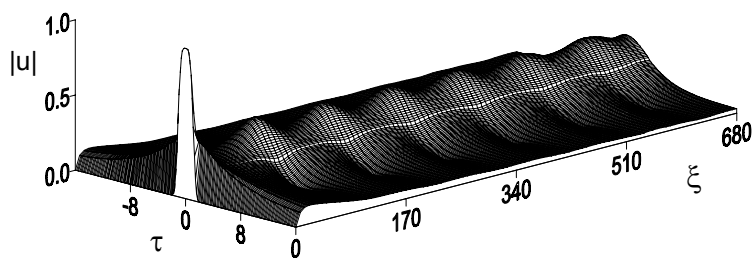
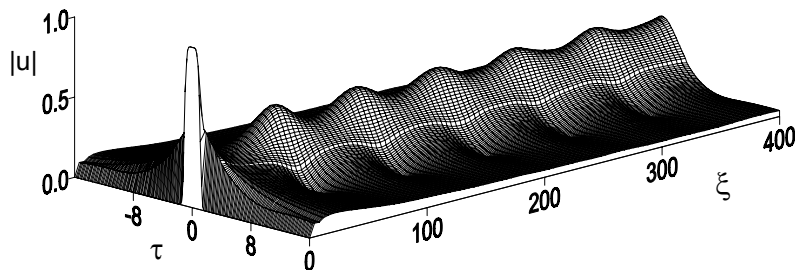Fig. 1. Evolution of the super-Gaussian pulse of the first kind for $C = 2$.

Fig. 2. Evolution of the super-Gaussian pulse of the second kind for $C = 2$.
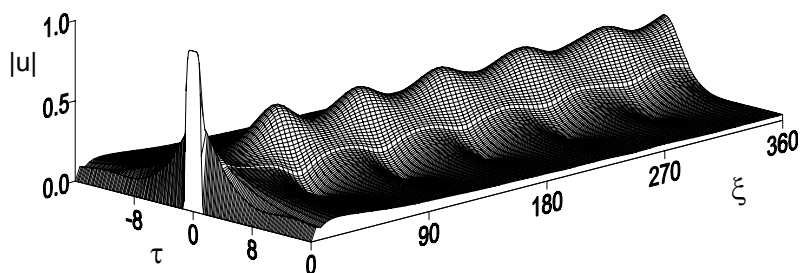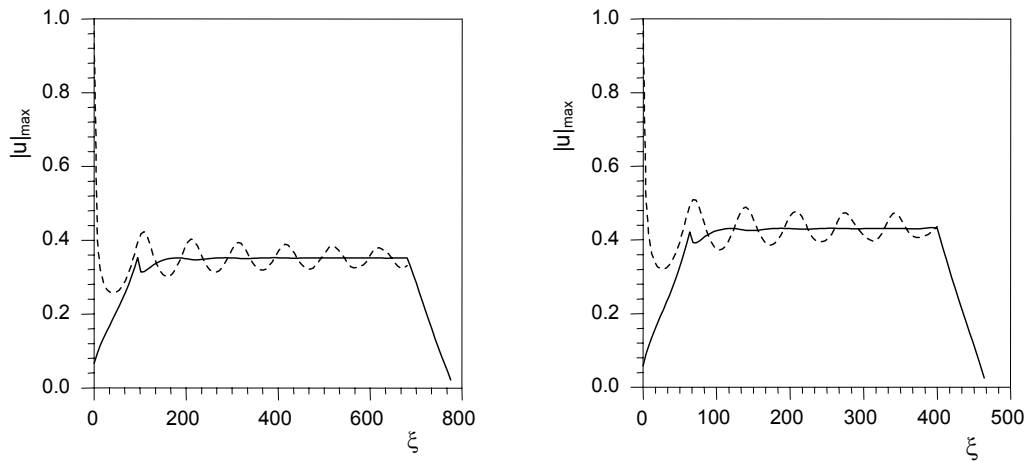

Fig. 3. Evolution of the super-Gaussian pulse of the third kind for $C = 2$.

– in the case of super-Gaussian pulse of the first kind ($m = 2$ in Eq. (8)): $C_{cr+} = 2.729$, $C_{cr-} = -2.736$;
– in the case of super-Gaussian pulse of the second kind ($m = 3$ in Eq. (8)): $C_{cr+} = 3.151$, $C_{cr-} = -3.159$;
– in the case of super-Gaussian pulse of the third kind ($m = 4$ in Eq. (8)): $C_{cr+} = 3.390$, $C_{cr-} = -3.406$.

4. Discussion

Figures 1–3 show the shape variation of the pulse as a function of the propagation distance for the value of the chirp parameter $C = 2$. Figure 1 concerns the case of the super-Gaussian pulse of the first kind initial shape. Figures 2 and 3 show the transformation of the super-Gaussian pulse of the second and third kind into soliton, respectively. The maximum influence of the nonlinearity can be seen at such points where the peak amplitude of the pulse reaches the local maximum (*i.e.*, the local narrowing of the pulse). On the contrary, the cumulation of the influence of the dispersion can be observed where the peak amplitude of the pulse reaches the local minimum (*i.e.*, the local broadening of the pulse). Variability of the peak amplitude value $|u|_{max}(\xi)$ of the pulse in the case of the super-Gaussian pulse of the first kind is presented as the dashed line in Fig. 4. The solid line (Fig. 4) illustrates the graphical interpretation of the functioning of the averaging filter, the use of which enables determination of the stationary peak amplitude value $|u|_{max, stationary}$ of the pulse for the

Fig. 4. Graphical interpretation of the averaging filter functioning; dashed line – evolution of the peak amplitude of the super-Gaussian pulse of the first kind (*i.e.*, the shape of the curve $|u|_{max}(\xi)$) for $C = 2$; solid line – current average of the curve $|u|_{max}(\xi)$.
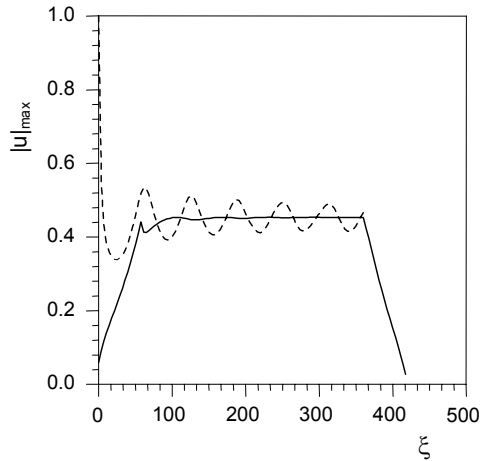
Fig. 5. Graphical interpretation of the averaging filter functioning; dashed line – evolution of the peak amplitude of the super-Gaussian pulse of the second kind (*i.e.*, the shape of the curve $|u|_{max}(\xi)$) for $C = 2$; solid line – current average of the curve $|u|_{max}(\xi)$.

Fig. 6. Graphical interpretation of the averaging filter functioning; dashed line – evolution of the peak amplitude of the super-Gaussian pulse of the third kind (*i.e.*, the shape of the curve $|u|_{max}(\xi)$) for $C = 2$; solid line – current average of the curve $|u|_{max}(\xi)$.

adequate value of the chirp parameter C. Figures 5 and 6 correspond to Fig. 4 except for the fact that Figs. 5 and 6 refer to the super-Gaussian pulse of the second and third kind, respectively. Making comparison between Figs. 1–3 as well as between Figs. 3–5 it can be noticed that for $C = 2$ the stationary peak amplitude value $|u|_{max, stationary}$ approaches zero faster in the case of super-Gaussian pulse of the first kind than in that of the second kind, and $|u|_{max, stationary}$ approaches zero faster in the
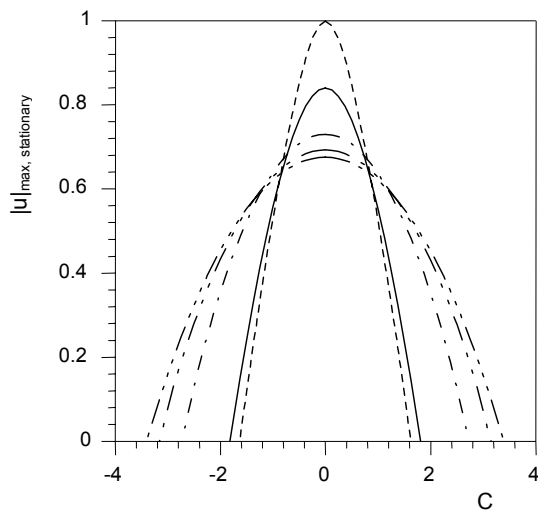

Fig. 7. Curve $|u|_{max, stationary}(C)$ in the case of: hyperbolic secant shape pulse – dashed line, Gaussian shape pulse – solid line, super-Gaussian pulse of the first kind – dotted line, super-Gaussian pulse of the second kind – double dotted line, super-Gaussian pulse of the third kind – triple dotted line.

case of super-Gaussian pulse of the second kind than in that of the third kind initial shape. This observations is confirmed and illustrated in Fig. 7, where the curves $|u|_{\text{max, stationary}}(C)$ in the case of hyperbolic secant, Gaussian, super-Gaussian pulse of the first, second and third kind are presented.

5. Conclusions

On the basis of the calculations performed it has been found that super-Gaussian shape is less sensitive to the destructive influence of the initial linear chirp than Gaussian pulse, and Gaussian shape is less sensitive to initial chirp than hyperbolic secant shape pulse. Furthermore the absolute values of the critical chirp parameter satisfy the following condition $|C_{\text{cr}+}| < |C_{\text{cr}-}|$. From the above condition there arises the fact that negative chirp is slightly less dangerous than positive one.

References

[1] AGRAWAL G.P., *Nonlinear Fiber Optics*, Academic Press, San Diego 1995.
[2] MAJEWSKI A., *Nieliniowa optyka światłowodowa. Zagadnienia wybrane*, WPW, Warszawa 1993 (in Polish).
[3] HAGEL R, ZAKRZEWSKI J., *Miernictwo dynamiczne*, WNT, Warszawa 1984 (in Polish).
[4] PRESS W.H., VATTERLING W.T., TEUKOLSKY S.A., FLANNERY B.P., *Numerical Recipes in Fortran 77*, Cambridge University Press 1992.